

Title	Reconstructing the model of a nonlinear MEMS structure by the example of a piezoelectric resonant energy harvester
Authors	Blokhina, Elena;O'Riordan, Eoghan;Olszewski, Oskar Zbigniew;Houlihan, Ruth;Mathewson, Alan;Bizzarri, Federico;Brambilla, Angelo
Publication date	2018-05-04
Original Citation	Blokhina, E., O'Riordan, E., Olszewski, O.Z., Houlihan, R., Mathewson, A., Bizzarri, F. and Brambilla, A. (2018) 'Reconstructing the model of a nonlinear MEMS structure by the example of a piezoelectric resonant energy harvester', 2018 IEEE International Symposium on Circuits and Systems (ISCAS), Florence, Italy, 27-30 May. doi:10.1109/ISCAS.2018.8351130
Type of publication	Conference item
Link to publisher's version	10.1109/ISCAS.2018.8351130
Rights	© 2018, IEEE. Personal use of this material is permitted. Permission from IEEE must be obtained for all other uses, in any current or future media, including reprinting/republishing this material for advertising or promotional purposes, creating new collective works, for resale or redistribution to servers or lists, or reuse of any copyrighted component of this work in other works.
Download date	2025-02-13 22:25:51
Item downloaded from	<a href="https://hdl.handle.net/10468/7201">https://hdl.handle.net/10468/7201</a>



# UCC

**University College Cork, Ireland**  
Coláiste na hOllscoile Corcaigh

# Reconstructing the Model of a Nonlinear MEMS Structure by the Example of a Piezoelectric Resonant Energy Harvester

Elena Blokhina  
and Eoghan O’Riordan  
University College Dublin  
Dublin, Ireland

Oskar Z. Olszewski, Ruth Houlihan  
and Alan Mathewson  
Tyndall National Institute  
Cork, Ireland

Federico Bizzarri  
and Angelo Brambilla  
Politecnico di Milano  
Milano, Italy

**Abstract**—Microelectromechanical systems contain mechanical elements coupled with conditioning electronics that control and process the signal generated by the mechanical component. These systems are miniature and can be easily integrated on one chip, which explains the enormous popularity of MEMS. The applications of MEMS began with environmental sensors and have grown to encompass RF and optical applications along with energy harvesting. Because of their mixed-domain nature, the design of conditioning electronics relies on accurate models of the mechanical component. As an additional requirement, the model must be simple enough and be compatible with common circuit simulation tools. The latter requirement may be particularly difficult to achieve due to the fact that most of modern MEMS structures are quite complex and often nonlinear. In this conference contribution, we describe the methodology of building a model of a nonlinear MEMS resonator using the conventional modelling approach and then using an improved model together with an optimisation technique on the basis of the circuit simulator PAN.

## I. INTRODUCTION

Microelectromechanical systems (MEMS) is a collective term for a broad range of systems and applications that integrate moving mechanical components and control electronics [1]. Among the most common applications for MEMS are inertial and environment sensors, microphones, optical switches and RF components [2]–[4]. Over recent years with the widespread development of the Internet of Things (IoT) and energy harvesting technology [5]–[8], various types of MEMS cantilevers have found applications in kinetic energy harvesting where they serve as elements capturing the motion of the environment [9]–[15].

Regardless of application, all MEMS have mechanical movable components and conditioning electronics that control and process the signal generated by the mechanical components. Hence, circuit design for MEMS has to follow certain constraints and limitations imposed by the behaviour of the mechanical component and the transduction mechanisms involved. The typical approach to design and model the mechanical component of MEMS is to employ a finite-element-method environment such as COMSOL or Coventor. On the other hand, one would rely on a conventional circuit simulation environment such as SPICE to design and model conditioning circuitry. A system level model, incorporating both the mechanical and circuit components is most commonly

done using SPICE (or MATLAB). The success of design for MEMS relies on the accuracy of models for their mechanical component [16]–[18]. As an additional requirement, the model must be simple enough and be compatible with common circuit simulation tools. The latter requirement may be particularly difficult to achieve since most modern MEMS structures are quite complex and often nonlinear [19]–[28].

With respect to the application of MEMS in energy harvesting, MEMS resonators have found their use in this field as elements that capture the motion of the environment or generate motion as a response to the environment. Micro-scale energy harvesters scavenge low amounts of energy from ambient environment and convert it to electricity. Energy harvesting is driven by the power requirements of the large number of electronic sensors that are anticipated to constitute the IoT. There are numerous transduction techniques to convert mechanical energy into electrical energy, notably piezoelectric, electromagnetic and electrostatic [11].

MEMS based energy harvesters stimulate the development of ultra-low power circuits [29]. A miniature harvester must be able to convert and store enough energy to power a sensor. However, the operation of a harvester and its power management requires power too. Since only a very small amount of the converted power is available, the harvester’s circuitry must operate in optimised mode. The design of such circuitry is a challenging task that requires a knowledge of the behaviour of the mechanical component. Hence we highlight again the importance to have an accurate and simple model of the MEMS mechanical component to ease its circuit design.

This paper aims at having a methodology to construct a lumped model for nonlinear MEMS resonators. As an example, we use a piezoelectric MEMS harvester. We discuss how to formulate its lumped model and a conventional approach to extract nonlinear coefficients appearing in the model from experimental data. We then present a new optimisation technique developed on the basis of the circuit simulator PAN combined with MATLAB into one environment. The improved procedure allows us not only to obtain the nonlinear stiffness coefficients but also to improve other parameters of the model. In this study, we also provide a discussion on the role of nonlinearities and provide a comparison of the proposed models with experimental results.

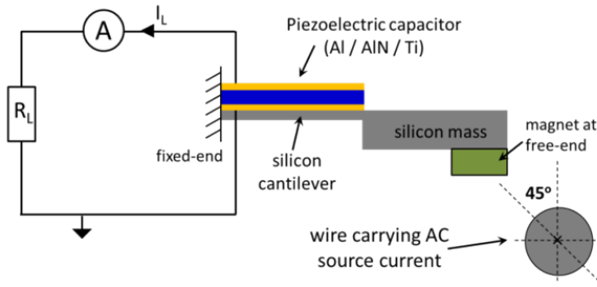


Figure 1. Schematic view of the piezoelectric harvester. The MEMS cantilever contains a magnet that responds to the current flowing in a wire. In the simplest case, the voltage generated across the cantilever is processed by a simple circuit consisting of a load resistor  $R_L$ . However in the most general case, the circuitry will be more advanced.

## II. BRIEF DESCRIPTION OF THE PIEZOMEMS ENERGY HARVESTER AND ITS FREQUENCY RESPONSE

The piezoelectric MEMS energy harvester that we use as an example in this paper is designed to scavenge energy from an AC current-carrying wire. It consists of a MEMS cantilever with a volume in the order of  $\text{cm}^3$  and operates at low frequencies (approx. 40 – 50 Hz). A permanent magnet is attached to the MEMS cantilever. As a result, the cantilever is excited by the force generated by coupling the magnet to an AC magnetic field due to a current flowing through a wire with low frequency oscillations ( $\omega_{\text{ext}} = 2\pi f_{\text{ext}}$ ). The schematic view of the device is shown in Fig. 1. The piezoelectric device converts the mechanical strain into a voltage that can be measured across the capacitor electrodes. The total length of the device is 10 mm, which includes a 1.5 mm long cantilever and an 8.5 mm long mass. The width of the device is 7 mm and the cavity etched in the mass is 6.5 mm along the device length by 5 mm along the width. The device was fabricated from a Silicon on Insulator (SOI) wafer with a  $17 \mu\text{m}$  thick device silicon layer, a  $1 \mu\text{m}$  thick buried oxide, and a  $535 \mu\text{m}$  thick bulk silicon [30], [31].

An experimental frequency sweep (i.e., the dependence of

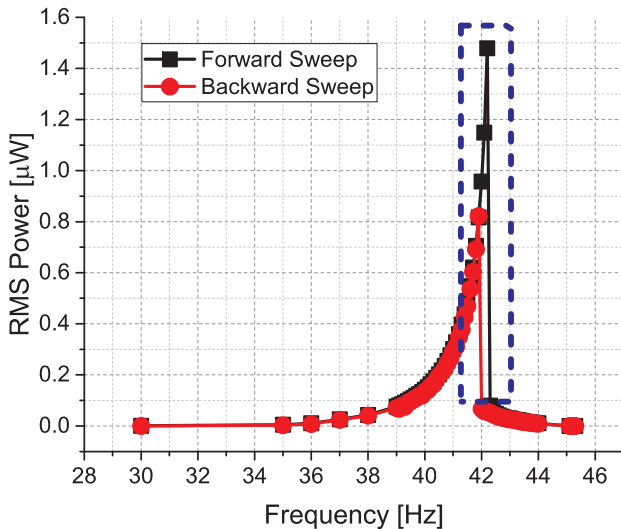


Figure 2. An experimental frequency sweep (i.e., the dependence of the RMS converted power vs. the frequency  $f_{\text{ext}}$ ). The response displays is overall hardening behaviour at large displacements of the piezoelectric beam.

the RMS converted power on the frequency  $f_{\text{ext}}$ ) is shown in Fig. 2. When discussing the behaviour in Fig. 2 (this qualitative behaviour is prevalent in many MEMS devices) we note a particular feature of interest to this study. There is an overall hardening response at large displacements of the piezoelectric beam [32]. In this context, ‘hardening’ refers to cases when the resonant frequency moves to higher frequencies than the natural frequency. We also note that multi-modality is one type of nonlinear behaviour which occurs in the presented device. Multi-modality occurs when, for the same external excitation and circuit parameters, more than one stable mode exists. This means that the device can highlight two (or more) dynamic behaviours, for example, with different amplitudes. The actual mode in which the system is in at a given moment depends on its history or on the initial conditions. This behaviour of nonlinear oscillators in the context of energy harvesting is widely discussed in the literature [14], [25], [33]–[35]. The two modes correspond to two different forced vibrations in the resonator, one with large amplitude and the other with smaller amplitude.

The circuit parameters such as  $R_L$  and the initial estimations of the device parameters that are particularly important for constructing its lumped model are given in Table I. These are obtained from the designed geometry of the resonator and are expected to be the case for the device. From the nonlinear response shown in Fig. 2, we also expect the presence of nonlinear stiffness coefficients, but these cannot be estimated in a straightforward fashion. The next two Sections describe the procedures we employ to obtain the lumped model of the MEMS device and extract the nonlinear coefficients.

Table I  
PARAMETERS OF THE MEMS DEVICE

Proof mass ( $m$ )	$7.36 \cdot 10^{-5} \text{ kg}$
Quality factor ( $Q$ )	59.5
Spring constant ( $k$ )	$4.65 \text{ N} \cdot \text{m}^{-1}$
Load Resistance ( $R_L$ )	$1.9 \cdot 10^6 \Omega$
Piezoelectric capacitance ( $C_p$ )	$2.1 \cdot 10^{-9} \text{ F}$

## III. FORMULATION OF THE NONLINEAR LUMPED MODEL AND EXTRACTION OF NONLINEAR COEFFICIENTS: CONVENTIONAL APPROACH

In this section we show an approach to construct a nonlinear lumped model of the MEMS device. The motion of the resonator displacement can be described by nonlinear, coupled differential equations driven by ambient vibrations. The resonator frame moves due to the external vibrations. The displacement  $x$  of the piezoelectric beam, with respect to the frame, is also affected by the transducer force  $f_t$  arising due to piezoelectric transduction:

$$m\ddot{x} + b\dot{x} + kx + \sum_{n=2}^N k_n x^n = mA_{\text{ext}} \cos \omega_{\text{ext}} t + f_t \quad (1)$$

where  $m$  is the mass of the resonator,  $b$  is the damping coefficient,  $k$  is the (linear) spring constant,  $k_n$  are the nonlinear stiffness coefficients,  $A_{\text{ext}}$  is the acceleration amplitude of external vibrations,  $\omega_{\text{ext}}$  is the external frequency and  $f_t$  represents the transducer force describing the coupling between the electrical and mechanical domains. In the most

general case, the transducer force depends on both electrical and mechanical states and on the design of the transducer. In this case, the transducer force is proportional to the generated voltage  $V$ :

$$f_t(x, V) = -\Omega V \quad (2)$$

Here we introduce a coupling factor, which was estimated from finite-element method simulations:  $\Omega = 3.2 \cdot 10^{-6} \text{ N} \cdot \text{V}^{-1}$ . The transducer force is the method by which the mechanical energy is converted into electrical energy. Thus, the force is different amongst piezoelectric, electromagnetic and electrostatic [10].

The experimental set-up was placed in series with a load resistance  $R_L$ . The governing equations describing the electrical behaviour of the simple conditioning circuitry are given by Kirchhoff's voltage law:

$$C_p \frac{dV}{dt} = \Omega \dot{x} - \frac{V}{R} \quad (3)$$

where  $V$  is the output voltage and  $C_p$  is the piezoelectric capacitance. Here a simple load resistance is used to mimic the load presented by a more complex conditioning and/or power management circuit [36].

The RMS power converted by the device is

$$P = V \cdot I_L = R_L I_L^2 \quad (4)$$

where  $I_L$  is the RMS (as measured by a multimeter) current generated in the circuit as shown in Fig. 1.

With the introduction of the nonlinear stiffness coefficients  $k_n$  in the model given by eq. (1), our task is to find these coefficients based on the experimental frequency response shown in Fig. 2. The main algorithm is as follows. It can be shown that mechanical nonlinearities that arise due to pre-existing mechanical strain in cantilevers would usually result in an odd spring force response such that  $f_{\text{spring}}^{\text{nonlin}}(x) = -f_{\text{spring}}^{\text{nonlin}}(-x)$ . Hence, following the conventional approach, we limit ourselves to odd terms in the expression for the nonlinear spring force in eq. (1), namely the third and fifth nonlinear

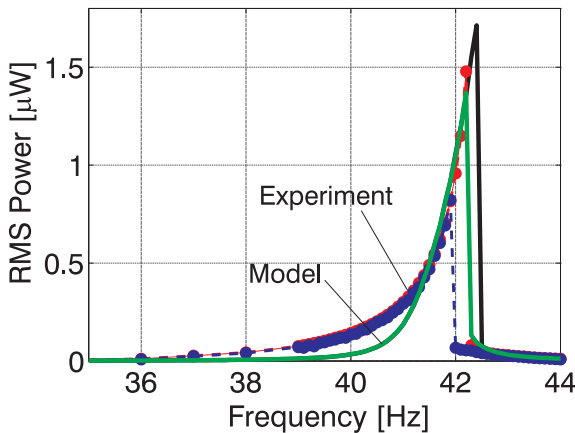


Figure 3. Comparison of the conventional nonlinear lumped model (forward sweep – continuous black line, backward sweep – continuous green line) with the nonlinear coefficients obtained through a numerical optimisation procedure with the experimental frequency sweep (forward sweep – red circles, backward sweep – blue circles).

coefficients  $k_3$  and  $k_5$ . We select different values of the nonlinear stiffness coefficients and solve the set of equations (1)-(3) numerically for a discrete set of external frequencies  $f_{\text{ext}}^{\{k\}}$ . Based on numerical simulations, a pair of  $k_3$  and  $k_5$  that leads to minimising the error  $\sum_k [P_{\text{RMS,experiment}}^{\{k\}} - P_{\text{RMS,simulated}}^{\{k\}}]^2$  is selected. As a result of this fully numerical optimisation procedure, we obtain the coefficient  $k_3$  and  $k_5$  listed in Table II.

Table II  
NONLINEAR STIFFNESS COEFFICIENTS

Nonlinear Spring Coefficient ( $k_3$ )	$8.3 \cdot 10^4 \text{ N} \cdot \text{m}^{-3}$
Nonlinear Spring Coefficient ( $k_5$ )	$-4.5 \cdot 10^9 \text{ N} \cdot \text{m}^{-5}$

Figure 3 shows the comparison of the nonlinear model (in terms of the RMS converted power vs. frequency  $f_{\text{ext}}$ ). It shows that the nonlinear model captures the major features of the response (such as overall hardening behaviour). However this comparison suggests that the nonlinearity displayed by the system is not adequately described by the cubic and fifth-order terms. For this reason, the next Section describes an improved model and the extraction of the nonlinear stiffness coefficients using the circuit simulator PAN.

#### IV. IMPROVED MODEL AND EXTRACTION OF COEFFICIENTS USING THE CIRCUIT SIMULATOR PAN

In this section, we revise the parameters of the harvester model described by expressions (1)-(3). An alternative optimisation procedure was carried out using the MATLAB-PAN (MP) environment. We propose that the mechanical model described in equation (1) should be modified to obtain a better matching between simulation and experimental results. The block diagram that concisely introduces the MP environment is shown in Fig. 4 [37].

The MP environment is composed of two main parts: MATLAB and the circuit simulator PAN [38]. MATLAB is the backplane to which the PAN simulation environment is linked through an external MEX shared library. PAN is a circuit simulator that admits the description of heterogeneous systems that can be described:

- At device level through a conventional SPICE-like netlist;
- As behavioural block through the VERILOG-A hardware description language;
- As a digital block through the VERILOG/VHDL description language;
- As a MATLAB procedure;
- By implementing the model equation in a conventional programming language such as for example C++ or FORTRAN.

The parameters of the devices can be accessed and modified from MATLAB and the analyses can be performed by MATLAB and results collected.

We have used the MP simulation environment to implement the nonlinear model of the studied MEMS device through a MATLAB function and the simple electrical circuit through a conventional SPICE-like netlist. This environment, while perhaps not necessary in this example with a simple electrical scheme, has been chosen with a view towards further work

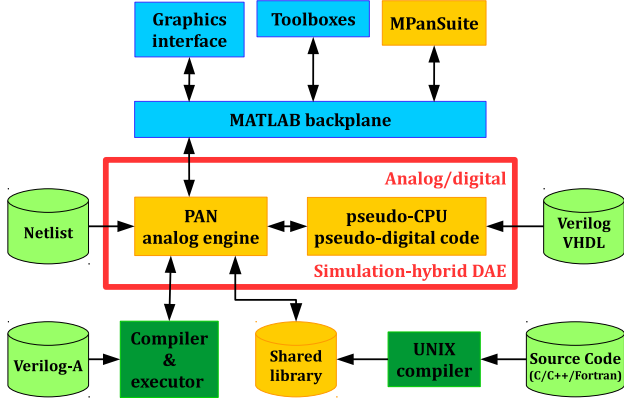


Figure 4. The block diagram showing the architecture of the MATLAB-PAN environment.

when we plan to add an additional power management circuit. This way, the modelling can be easily and efficiently done in PAN. MATLAB makes available a large set of in-built efficient and powerful optimisation algorithms. The objective is the minimisation of the errors between the simulated and measured root mean square values (RMSs) of the power dissipated across the  $R_L$  load resistor on a set of discrete frequencies of the external driving force (the  $\cos(\omega_{\text{ext}})$  function in (1)). We run the optimisation method in MATLAB, at each iteration it alters the parameters of the MEMS harvester and a shooting analysis is performed by the circuit simulator to compute the steady-state working condition of the MEMS harvester. The RMS of the simulated current is thus computed and the converted power is calculated. The optimisation procedure described in this Section finds not only the nonlinear stiffness coefficients  $k_3$  and  $k_5$  but also improves other parameters of the model including the coupling coefficient  $\Omega$ , the quality factor  $Q$  (which is related to the damping coefficient  $b$ ), etc.

In order to achieve better optimisation results, we suggest that one modifies the mechanical model in expression (1) by imposing that all terms in the summation are odd functions. Hence, eq. (1) is rewritten as

$$m\ddot{x} + b\dot{x} + kx + \sum_{n=1}^N k_{2n} |x| x^{2n-1} + \sum_{n=1}^N k_{2n+1} x^{2n+1} = m A_{\text{ext}} \cos(\omega_{\text{ext}} t) + f_t \quad (5)$$

Here we limit the sum to  $N = 2$  meaning that we introduce four nonlinear coefficients  $k_{2,3,4,5}$ .

The optimisation flow starts by optimising the values of the RMS power at the lower and upper extremes of the frequency interval. In these extremes, the harvester behaves as an almost linear element and thus we expect to accurately fit the values of the  $b$  (or  $Q$ ),  $k$  and  $\Omega$  parameters. We set to 0 the  $k_i$  parameters of the series in (1). We then perform a new optimisation by starting from the previous values of the parameters and introducing the new  $k_2$  parameter. The optimisation process is cycled by adding the  $k_3$ ,  $k_4$  and finally  $k_5$  terms in the summation. A final optimisation is performed with all the mentioned parameters including  $A_{\text{ext}}$ . In Fig. 5 we report the results of the optimisation of the improved model and the comparison with the experimental result.

Table III  
EXTRACTED COEFFICIENTS OF THE IMPROVED NONLINEAR MODEL

$Q$	63.55	$k$	$4.65 \text{ N} \cdot \text{m}^{-1}$
$k_2$	$6.53 \cdot 10^2 \text{ N} \cdot \text{m}^{-2}$	$k_3$	$4.14 \cdot 10^4 \text{ N} \cdot \text{m}^{-3}$
$k_4$	$-1.56 \cdot 10^8 \text{ N} \cdot \text{m}^{-4}$	$k_5$	$-4.01 \cdot 10^9 \text{ N} \cdot \text{m}^{-5}$
$\Omega$	$4.34 \cdot 10^{-6} \text{ N} \cdot \text{V}^{-1}$	$A_{\text{ext}}$	$0.18g$

We note that during the first phase of the optimisation (the one that optimises the parameters of the almost linearly behaving MEMS harvester) the extremes of the RMS power versus frequencies curve are well fitted. The fitting of the  $k_2$  term deforms the curve that better adheres to the experimental one in the frequency range where the values of the RMS power are higher. The peak value is not adequately fitted. The introduction and fitting of the  $k_3$ ,  $k_4$  and  $k_5$  parameters gives a very good result where the simulation curve almost perfectly overlaps the experimental one and falls exactly at the same frequency value. Simulation shows that different stable and unstable periodic solutions coexist and that the system “jumps” from a stable solution to a different one during variations of the frequency of the excitation force.

## V. CONCLUSIONS

This work uses a nonlinear piezoelectric MEMS device as an example for a methodology to construct a nonlinear lumped model. The frequency response demonstrated by the studied MEMS cantilever is very typical for a broad class of oscillating MEMS devices. Hence, the results we have obtained can be generally expanded to other classes of microsystems. We began by discussing the nonlinear features of the frequency response and proposing a conventional lumped model of the device. The nonlinear stiffness coefficient for the conventional model were obtained through straightforward numerical simulations and their comparison with the experimental frequency response. We then proceed to an improved nonlinear model and describe an optimisation procedure with the MATLAB-PAN environment. This procedure allowed us to extract the nonlinear stiffness coefficients and improve the values of other parameters utilised in the model.

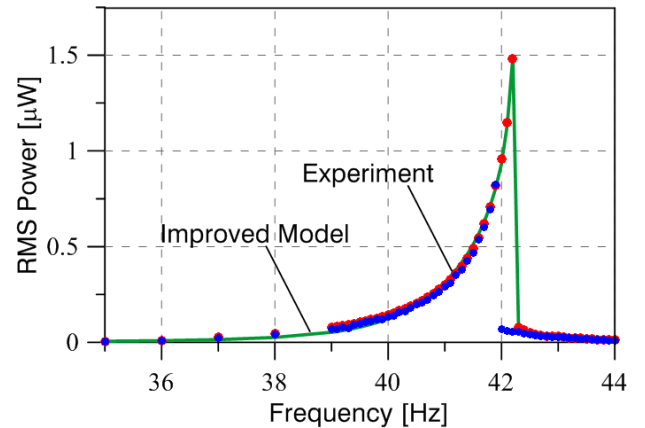


Figure 5. The result of the optimisation procedure with the MATLAB-PAN environment. Comparison of the improved nonlinear lumped model (continuous green line) with the experimental frequency sweep (forward sweep – red circles, backward sweep – blue circles)

## REFERENCES

- [1] S. D. Senturia, *Microsystem design*. Springer Science & Business Media, 2007.
- [2] C. Liu, *Foundations of MEMS*. Pearson Education India, 2012.
- [3] S. Lucyszyn, *Advanced RF Mems*. Cambridge University Press, 2010.
- [4] S. Tadigadapa and K. Mateti, "Piezoelectric MEMS sensors: state-of-the-art and perspectives," *Measurement Science and Technology*, vol. 20, no. 9, p. 092001, 2009.
- [5] M. H. Miraz, M. Ali, P. S. Excell, and R. Picking, "A review on internet of things (IoT), internet of everything (IoE) and internet of nano things (IoNT)," in *Internet Technologies and Applications (ITA), 2015*, 2015, pp. 219–224.
- [6] S. Kim, R. Vyas, J. Bitto, K. Niotaki, A. Collado, A. Georgiadis, and M. M. Tentzeris, "Ambient RF energy-harvesting technologies for self-sustainable standalone wireless sensor platforms," *Proceedings of the IEEE*, vol. 102, no. 11, pp. 1649–1666, 2014.
- [7] R. J. Vullers, R. Van Schaijk, H. J. Visser, J. Penders, and C. Van Hoof, "Energy harvesting for autonomous wireless sensor networks," *IEEE Solid-State Circuits Magazine*, vol. 2, no. 2, pp. 29–38, 2010.
- [8] P. Mitcheson, E. Yeatman, G. Rao, A. Holmes, and T. Green, "Energy harvesting from human and machine motion for wireless electronic devices," *Proceedings of the IEEE*, vol. 96, no. 9, pp. 1457–1486, 2008.
- [9] P. Basset, E. Blokhina, and D. Galayko, *Electrostatic kinetic energy harvesting*. John Wiley and Sons, 2016.
- [10] E. Blokhina, A. El Aroudi, E. Alarcon, and D. Galayko, *Nonlinearity in Energy Harvesting Systems: Micro-and Nanoscale Applications*. Springer, 2016.
- [11] O. Brand, G. K. Fedder, C. Hierold, J. G. Korvink, and O. Tabata, *Micro energy harvesting*. John Wiley & Sons, 2015.
- [12] S.-G. Kim, S. Priya, and I. Kanno, "Piezoelectric MEMS for energy harvesting," *MRS Bulletin*, vol. 37, no. 11, pp. 1039–1050, 2012.
- [13] H. Li, C. Tian, and Z. D. Deng, "Energy harvesting from low frequency applications using piezoelectric materials," *Applied physics reviews*, vol. 1, no. 4, p. 041301, 2014.
- [14] P. Basset, D. Galayko, F. Cottone, R. Guillemet, E. Blokhina, F. Marty, and T. Bourouina, "Electrostatic vibration energy harvester with combined effect of electrical nonlinearities and mechanical impact," *Journal of Micromechanics and Microengineering*, vol. 24, no. 3, p. 035001, 2014.
- [15] S. P. Beeby, R. Torah, M. Tudor, P. Glynne-Jones, T. O'Donnell, C. Saha, and S. Roy, "A micro electromagnetic generator for vibration energy harvesting," *Journal of Micromechanics and Microengineering*, vol. 17, no. 7, p. 1257, 2007.
- [16] S. F. Bart, T. A. Lober, R. T. Howe, J. H. Lang, and M. F. Schlecht, "Design considerations for micromachined electric actuators," *Sensors and Actuators*, vol. 14, no. 3, pp. 269–292, 1988.
- [17] L. R. Carley, G. Ganger, D. F. Guillou, and D. Nagle, "System design considerations for MEMS-actuated magnetic-probe-based mass storage," *IEEE Transactions on Magnetics*, vol. 37, no. 2, pp. 657–662, 2001.
- [18] M. Schwarz, J. Franz, and M. Reimann, "The future is MEMS design considerations of microelectromechanical systems at bosch," in *International Conference on Mixed Design of Integrated Circuits and Systems (MIXDES)*. IEEE, 2015, pp. 177–180.
- [19] F. Cottone, H. Vocca, and L. Gammaitoni, "Nonlinear energy harvesting," *Physical Review Letters*, vol. 102, no. 8, p. 080601, 2009.
- [20] S. C. Stanton, C. C. McGehee, and B. P. Mann, "Nonlinear dynamics for broadband energy harvesting: Investigation of a bistable piezoelectric inertial generator," *Phys. D: Nonlin. Phenom.*, vol. 239, pp. 640–653, 2010.
- [21] M. Marzencki, M. Defosseux, and S. Basrour, "MEMS vibration energy harvesting devices with passive resonance frequency adaptation capability," *IEEE Journal of Microelectromechanical Systems*, vol. 18, no. 6, pp. 1444–1453, 2009.
- [22] S. D. Nguyen and E. Halvorsen, "Nonlinear springs for bandwidth-tolerant vibration energy harvesting," *IEEE Journal of Microelectromechanical Systems*, vol. 20, pp. 1225–1227, 2011.
- [23] L.-C. J. Blystad and E. Halvorsen, "A piezoelectric energy harvester with a mechanical end stop on one side," *Microsystem Technologies*, vol. 17, no. 4, pp. 505–511, 2011.
- [24] M. Soliman, E. Abdel-Rahman, E. El-Saadany, and R. Mansour, "A wideband vibration-based energy harvester," *Journal of Micromechanics and Microengineering*, vol. 18, p. 115021, 2008.
- [25] P. Podder, A. Amann, and S. Roy, "Combined effect of bistability and mechanical impact on the performance of a nonlinear electromagnetic vibration energy harvester," *IEEE/ASME Transactions on Mechatronics*, vol. 21, no. 2, pp. 727–739, 2016.
- [26] C. P. Le and E. Halvorsen, "MEMS electrostatic energy harvesters with end-stop effects," *Journal of Micromechanics and Microengineering*, vol. 22, no. 7, p. 074013, 2012.
- [27] B. D. Truong, C. P. Le, and E. Halvorsen, "Experimentally verified model of electrostatic energy harvester with internal impacts," in *IEEE International Conference on Microelectromechanical Systems (MEMS)*, Jan 2015, pp. 1125–1128.
- [28] Y. Lu, E. Oriordan, F. Cottone, S. Boisseau, D. Galayko, E. Blokhina, F. Marty, and P. Basset, "A batch-fabricated electret-biased wideband MEMS vibration energy harvester with frequency-up conversion behavior powering a UHF wireless sensor node," *Journal of Micromechanics and Microengineering*, vol. 26, no. 12, p. 124004, 2016.
- [29] G. A. Rincón-Mora and S. Yang, "Tiny piezoelectric harvesters: Principles, constraints, and power conversion," *IEEE Transactions on Circuits and Systems I: Regular Papers*, vol. 63, no. 5, pp. 639–649, 2016.
- [30] O. Z. Olszewski, R. Houlihan, A. Mathewson, and N. Jackson, "A low frequency mems energy harvester scavenging energy from magnetic field surrounding an ac current-carrying wire," in *Journal of Physics: Conference Series*, vol. 757, no. 1. IOP Publishing, 2016, p. 012039.
- [31] O. Z. Olszewski, R. Houlihan, A. Blake, A. Mathewson, and N. Jackson, "Evaluation of vibrational PiezoMEMS harvester that scavenges energy from a magnetic field surrounding an AC current-carrying wire," *IEEE Journal of Microelectromechanical Systems*, 2017.
- [32] I. Kovacic and M. J. Brennan, *The Duffing equation: nonlinear oscillators and their behaviour*. John Wiley & Sons, 2011.
- [33] D. Nguyen, E. Halvorsen, G. Jensen, and A. Vogl, "Fabrication and characterization of a wideband MEMS energy harvester utilizing nonlinear springs," *Journal of Micromechanics and Microengineering*, vol. 20, no. 12, p. 125009, 2010.
- [34] D. Mallick, A. Amann, and S. Roy, "Interplay between electrical and mechanical domains in a high performance nonlinear energy harvester," *Smart Materials and Structures*, vol. 24, no. 12, p. 122001, 2015.
- [35] E. Oriordan, D. Galayko, P. Basset, and E. Blokhina, "Complete electromechanical analysis of electrostatic kinetic energy harvesters biased with a continuous conditioning circuit," *Sensors and Actuators A: Physical*, vol. 247, pp. 379–388, 2016.
- [36] M. Bedier and D. Galayko, "Multiple energy-shot load interface for electrostatic vibrational energy harvesters," in *IEEE International Conference on New Circuits and Systems Conference (NEWCAS)*, 2016, pp. 1–4.
- [37] F. Bizzarri and A. Brambilla, "PAN and MPanSuite: Simulation vehicles towards the analysis and design of heterogeneous mixed electrical systems," in *IEEE International Conference of New Generation of Circuits and Systems (NGCAS)*, Sept 2017, pp. 1–4.
- [38] F. Bizzarri, A. Brambilla, G. Storti Gajani, and S. Banerjee, "Simulation of real world circuits: Extending conventional analysis methods to circuits described by heterogeneous languages," *IEEE Circuits and Systems Magazine*, vol. 14, no. 4, pp. 51–70, 2014.